



Few Band Astrophysical Parameter Estimation - **Priam: Photometric Estimation of Astrophysical Parameters**

prepared by: Dae-Won Kim
reference: GAIA-C8-TN-MPIA-DWK-001
issue: 1
revision: 0
date: 2013-03-13
status: Issued

Abstract

This is a technical note for astrophysical parameter (AP) estimation using two or three colors derived from integrated BP/RP flux. We tested two machine learning algorithms including Support Vector Machine and Gaussian Process to estimate APs. The results comparing two methods are presented.

Document History

Issue	Revision	Date	Author	Comment
1	0	2013-03-13	DWK	First Draft

Contents

1	Introduction	5
1.1	Acronyms	5
2	Method	5
2.1	Regression Using Machine Learning	5
2.2	Experiments on Prior Application	6
3	Training a Model	6
3.1	Dataset	6
3.2	Training and Test Set	9
3.3	Tuning Parameters	9
3.4	Performance	10
3.4.1	Experiments Using Noise Added Samples	13
3.4.2	Experiments Using Uniformly Distributed Samples	13
3.4.3	Extrapolated Application to Samples of Extinction > 2.0 mag and of High Temperature $> 10,000\text{K}$	16
3.5	Application of Prior	16
3.5.1	Likelihood	18
3.5.2	Realistic Prior for Extinction and Temperature	19
3.5.3	Experimental Prior for Extinction and Temperature	23
3.5.4	Posterior	24
4	Implementation	27
<hr/> Technical Note		3

5 Conclusion and Discussion

28

1 Introduction

In this technical note, we present a preliminary results of AP estimation (i.e. extinction and temperature) using three (or two) color information including $G_{Mag} - G_{BP}$, $G_{Mag} - G_{RP}$ and/or $G_{Mag} - G_{RVS}$. A quick study on this subject is done by Bailer-Jones (2011) with/without prior on color, parallax, HRD, and extinction. See CBJ-064 and also a presentation pdf from the meeting. Please contact with Coryn Bailer-Jones or Dae-Won Kim for the results of the work.

The predicted APs would be useful early in mission when there are no BP/RP spectra available. Only G_{Mag} and integrated BP/RP photometry (hereinafter, G_{BP} and G_{RP}) will be released at the early stage in the mission (i.e. 28 months after the launch). Thus it would be nice to provide predicted APs using G_{Mag} , G_{BP} , G_{RP} and also G_{RVS} for bright stars (CBJ-064).

1.1 Acronyms

The following table has been generated from the on-line Gaia acronym list:

Acronym	Description
AP	Astrophysical Parameter
BP	Blue Photometer
DSC	Discrete Source Classification (Classifier)
GSPPHOT	Generalised Stellar Parametrised PHOTometry
HRD	Hertzsprung-Russell Diagram
MSC	Multiple-Star Classifier
QSO	Quasi-Stellar Object
RP	Red Photometer
SDSS	Sloan Digital Sky Survey
SVM	Support Vector Machine

2 Method

2.1 Regression Using Machine Learning

To estimate extinction and temperature using colors, we employed two machine learning algorithms including Support Vector Machine (SVM) and Gaussian Process (GP). These algorithms are capable of training either a classification model or a regression model using input dataset with known labels or output values.

SVM (Cortes & Vapnik, 1995) has been very popular for many years and successfully solved lots of classification/regression problems, and also have been used for many astronomical studies such as redshift estimation of galaxies, QSO selection, variable star classification, morphological galaxy separation, and etc. It is widely known that SVM is one of the most powerful and successful machine learning algorithms. Gaia CU8 group is also using SVM for DSC, MSC, and GSPPHOT (Liu et al., 2012).

GP (Bishop, 2006; Rasmussen & Williams, 2006) is a relatively new technique but it has becoming popular since the last decade, and also known to be very successful for classification and regression. One of the advantages of GP over SVM is that there are fewer kernel parameters to be tuned. In the case of SVM regression, one should tune three parameters (i.e. C , γ , and either ϵ or ν) while in the case of GP, there are two parameters including a length scale of kernel (l) and the maximum number of basis vector. Moreover, performance of GP is not significantly varying according to the number of basis vectors thus one actually needs to focus on tuning only one parameter, l . However GP is rather slower to train a model than SVM.

2.2 Experiments on Prior Application

As we only have a limited number of bands such as G_{RVS} , G_{Mag} , G_{BP} , G_{RP} , we do not have sufficient input parameters to precisely estimate APs. Thus in order to further constrain (or improve) AP estimation, we applied priors both for extinction and temperature. Details are given at Section 3.5.

3 Training a Model

In this section, we briefly introduce a dataset and how we tuned parameters in order to optimize regression models.

3.1 Dataset

We used MainDelivery3 PHOENIX RAN1 G150 library (noise-free) to build a training and test set. The library is from the cycle8 simulation and in MDB version 11. We first extracted the entire 14,000 samples from the library and then selected a subset consisting of the samples whose extinctions are smaller than or equal to 2. The total number of samples in the subset is 6,528.

Note that the extinction map of our galaxy generated using 65,000 M-dwarf spectra from SDSS has an extinction range between 0 and 2 (see Figure 1).¹ Thus, although we constrained our samples with extinction ≤ 2 , trained models based on these samples can be used to estimate

¹The work is done by Jones et al. (2011) using the SDSS spectra.

extinction and temperature for stellar objects that are in fact the dominant sources in our galaxy.

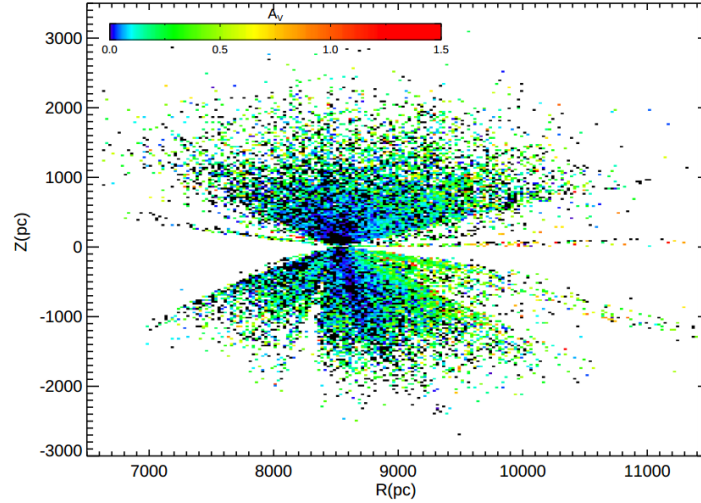


FIGURE 1: Extinction map generated using 65,000 M-dwarf spectra in our galaxy (Figure 6 from Jones et al. (2011))

Figure 2 shows distribution of extinction and temperature of these 6,528 samples. Since we cut the samples with extinctions ≤ 2 , the extinction histogram has a range between 0 and 2. Temperatures are between 3,000K and 10,000K.

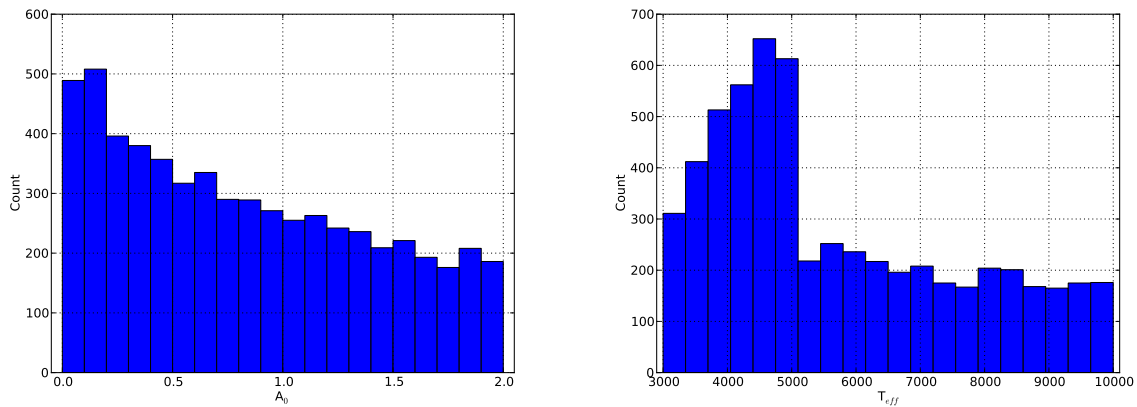


FIGURE 2: Histogram of extinction and temperature.

Figure 3 shows scatter plots of a relation between $G_{Mag} - G_{BP}$ versus extinction (temperature) color coded with temperature (extinction). As the figures show, temperature and extinction is highly degenerated in the color space. Thus an accuracy for estimation of extinction and temperature using colors is expected to be low. We also show 3D plots of extinction (temperature) versus three colors in Figure 4. Each axis is $G_{Mag} - G_{BP}$, $G_{Mag} - G_{RP}$ and $G_{Mag} - G_{RVS}$.

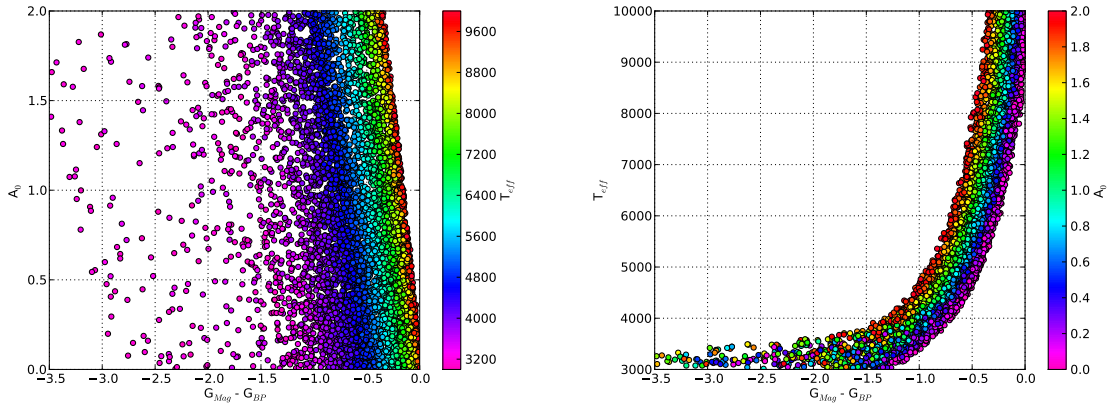


FIGURE 3: Scatter plot of $G_{Mag} - G_{BP}$ versus extinction (temperature). Color coded with temperature (extinction).

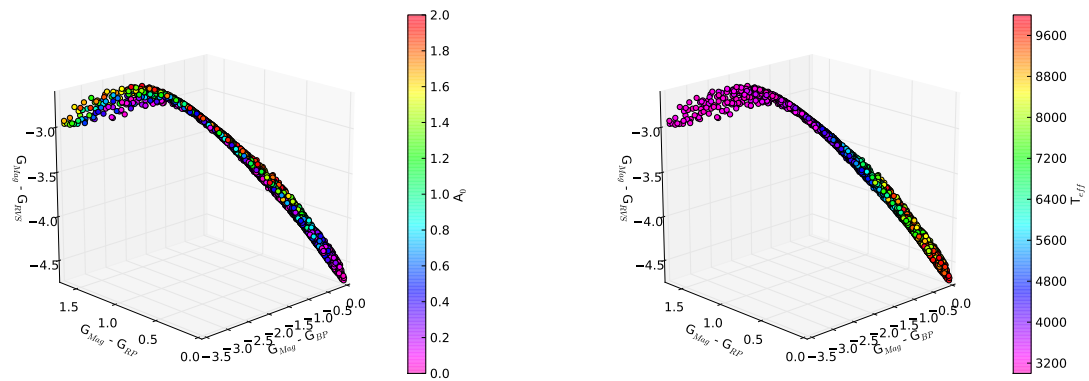


FIGURE 4: 3D plot of extinction (temperature) versus three colors. Each axis is $G_{Mag} - G_{BP}$, $G_{Mag} - G_{RP}$ and $G_{Mag} - G_{RVS}$.

In addition, Figure 5 shows a relation between extinction and temperature. As the figure shows, there is no correlation between the two APs in the entire dataset.

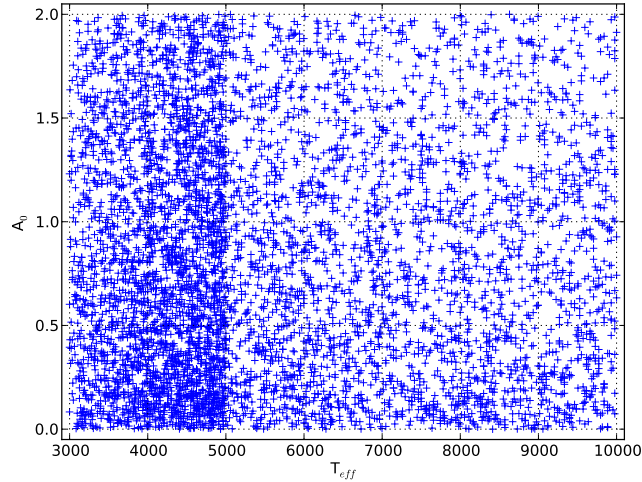


FIGURE 5: Scatter plot of extinction and temperature.

3.2 Training and Test Set

Using the selected subset including 6,528 samples, we build a training and a test set. The training set consists of randomly selected 5,222 samples (80%) and the test set consists of the remaining samples (1,306 samples, 20%). The training set is used to tune the model parameters of each method (Section 3.3) and the test set is used to estimate the performance (Section 3.4).

3.3 Tuning Parameters

In order to find the best parameter for SVM and GP model training, we used a grid search technique using 10x10 grid and 10-fold cross validation. Note that we used only the training set mentioned in the previous section. We did not use the test set at this stage. For the grid search, we repeated the search using a finer grid until the performance did not improve anymore. The parameter ranges we tested for each method are shown in Table 2. We used a radial basis function (rbf) as a kernel for both SVM and GP. In the case of SVM, we used ν -SVM Regression (ν -SVR), thus we needed to select the best ν parameter as well. We also used a grid search to select ν showing the best performance.

Figure 6 shows contour maps of performances² derived during the 10-fold cross validation

²We show the root mean squared (RMSE) error in the case of temperature. RMSE equation is given in the next section.

TABLE 2: Parameter ranges for the grid search

SVM		
rbf width	$0.001 \leq \gamma \leq 2$	
soft margin	$0.1 \leq C \leq 1000$	
GP		
length scale	$0.01 \leq l \leq 1$	
max. number of basis vector	$50 \leq N_v \leq 200$	

processes of each method. The left panel is the performance of SVM in the entire range of the tuning parameters. The SVM performance still increased after the range of tuning parameters but the performance gain was negligible. This could happen when a training data is noisy so that SVM tends to do overfitting the data. In general, γ (C) for either classification or regression is smaller than 1 (100). Nevertheless we select the maximum γ and C in the parameter range as the best parameters. The right panel is the performance of GP. Although more basis vectors give better results, the performance gain was negligible after 200 basis vectors. On contrary to SVM, GP converges at $l \sim 0.11$.

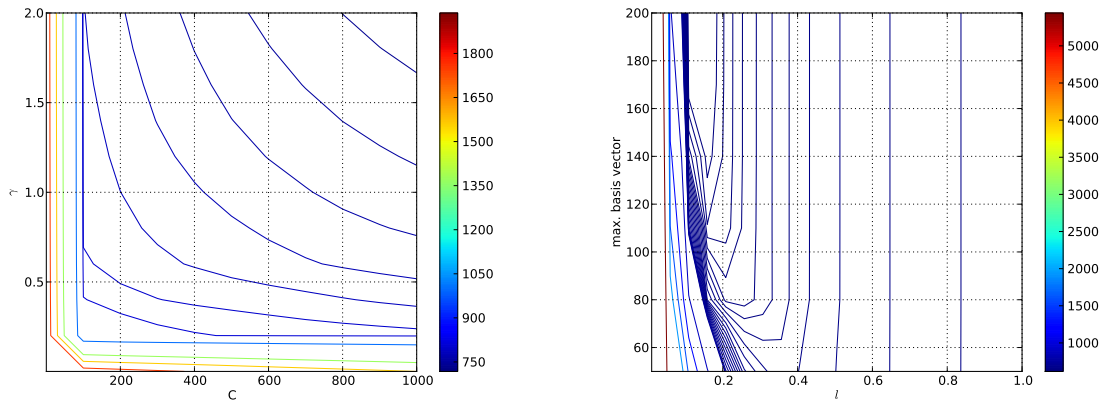


FIGURE 6: Performance (i.e. normalized root mean squared error) of each method according to the tuning parameters. left: SVM, right: GP. See the text for details.

3.4 Performance

We applied the trained models to the test set mentioned in Section 3.1. Since we did not use the test set to train the models, we can derive relatively reliable and unbiased performance. Table 3 shows two performance values derived using the test set. One is the root mean square error (RMSE) calculated as:

TABLE 3: Performance using three colors

Method	AP	RMSE	MAE
SVM	extinction	0.34 (mag)	0.27 (mag)
	temperature	706 (K)	509 (K)
GP	extinction	0.33 (mag)	0.26 (mag)
	temperature	629 (K)	429 (K)

Note that the distribution of temperature (Figure 2) shows that a large portion of samples have temperatures lower than 5,000K. Thus the performance for temperature could be biased to those samples.

TABLE 4: Prior-only MAE

extinction	temperature
0.50	1641

Prior-only MAE which can be understood as the upper limit of errors.

$$RMSE = \sqrt{\frac{1}{N} \sum_{i=1}^N (x_i^T - x_i^P)^2} \quad (1)$$

where N is the total number of samples in the test set, i is the index of each sample, x^T is the true value of APs and x^P is the predicted value of APs. An another performance value is the mean absolute error (MAE) calculated as:

$$MAE = \frac{1}{N} \sum_{i=1}^N |x_i^T - x_i^P| \quad (2)$$

As the table shows, GP's performance is slightly better than SVM's.

In Table 4 shows prior-only MAE (see Section 5.1 Liu et al. (2012) for details). It gives an idea of the upper limit of errors. All MAE values in Table 3 are smaller than these upper limit of errors, which implies the predicted APs are useful.

Figure 7 shows comparing results between the true APs and the predicted APs. For each subplot in the figure, the top panel is a relation between the true APs versus the predicted APs, and the bottom panel is residuals (i.e. true - predicted).

In addition, we show performance of AP estimation using only two colors of G_{Mag} , G_{BP} and G_{RP} (Table 5) since G_{RVS} would not be available for faint stars. Although the overall perfor-

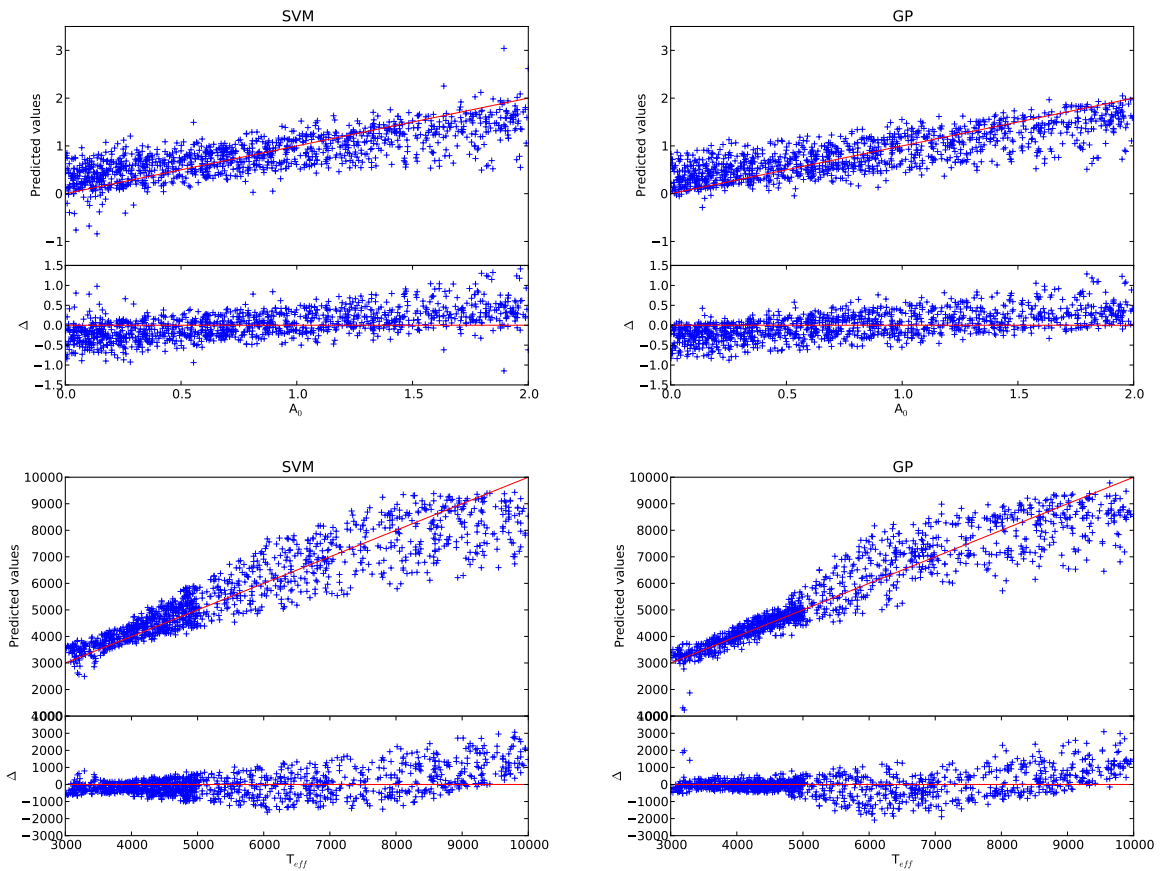


FIGURE 7: A scatter plot of the true APs and the predicted APs. In each subplot, top panel shows a relation between them and the bottom plot shows residuals (i.e. true - predicted). The red line in the top panel is a function of $y = x$ and the red line in the bottom panel is function of $y = 0$. Top left: extinction estimation using SVM, top right: extinction estimation using GP, bottom left: temperature estimation using SVM, and bottom left: temperature estimation using GP.

TABLE 5: Performance using two colors

Method	AP	RMSE	MAE
SVM			
	extinction	0.45 (mag)	0.36 (mag)
	temperature	769 (K)	578 (K)
GP			
	extinction	0.43 (mag)	0.34 (mag)
	temperature	676 (K)	490 (K)

mances are lower than the performances using three colors, the predicted APs might be still useful at early in the mission. Nevertheless, hereinafter we will only show three color results.

3.4.1 Experiments Using Noise Added Samples

In this section, we present performances using noise added samples. Except using artificially added noise samples, all other settings are identical with the experiments shown in the previous sections.

We performed experiments with each different magnitude of $G_{Mag} = 15, 18.5$ and 20 . Table 6 shows the results. Note that we did not optimize the kernel parameters for each cases but used the same ones selected from the previous section. Nevertheless, it would anyway yield the potentially best predictions.

As the table shows, the performances are worse at the fainter magnitude. However the performance of $G_{Mag} = 15$ is not very different from the performance from Table 3 since the noise level at $G_{Mag} = 15$ is almost negligible.

3.4.2 Experiments Using Uniformly Distributed Samples

As Figure 2 shows, the distribution of temperatures of samples are not uniform. Thus due to the nonuniform distribution of the samples, the performance could be affected. Although we do not know the true distribution of temperatures of samples that the Gaia satellite will observe, it is worth checking if different distribution of samples affect the performance.

We selected samples so their temperatures are uniformly distributed as shown in Figure 8. Table 7 shows the performance. As the table shows, overall performance are decreased. Table 8 shows prior-only MAE for these samples.

In Figure 9, we show the comparison results between the true APs and the predicted APs.

TABLE 6: Performance using noise added samples

Method	Magnitude	AP	RMSE	MAE
SVM				
	15	extinction	0.35 (mag)	0.27 (mag)
		temperature	706 (K)	508 (K)
	18.5	extinction	0.37 (mag)	0.29 (mag)
		temperature	708 (K)	511 (K)
	20	extinction	0.43 (mag)	0.35 (mag)
		temperature	727 (K)	533 (K)
GP				
	15	extinction	0.33 (mag)	0.26 (mag)
		temperature	628 (K)	429 (K)
	18.5	extinction	0.36 (mag)	0.28 (mag)
		temperature	641 (K)	443 (K)
	20	extinction	0.41 (mag)	0.35 (mag)
		temperature	685 (K)	493 (K)

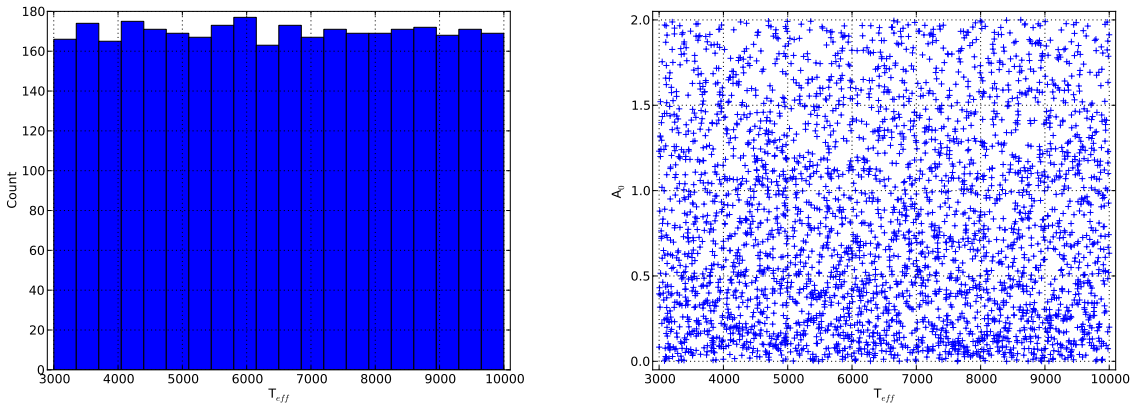


FIGURE 8: Left: histogram of uniformly distributed temperature samples. right: scatter plot of temperature and extinction.

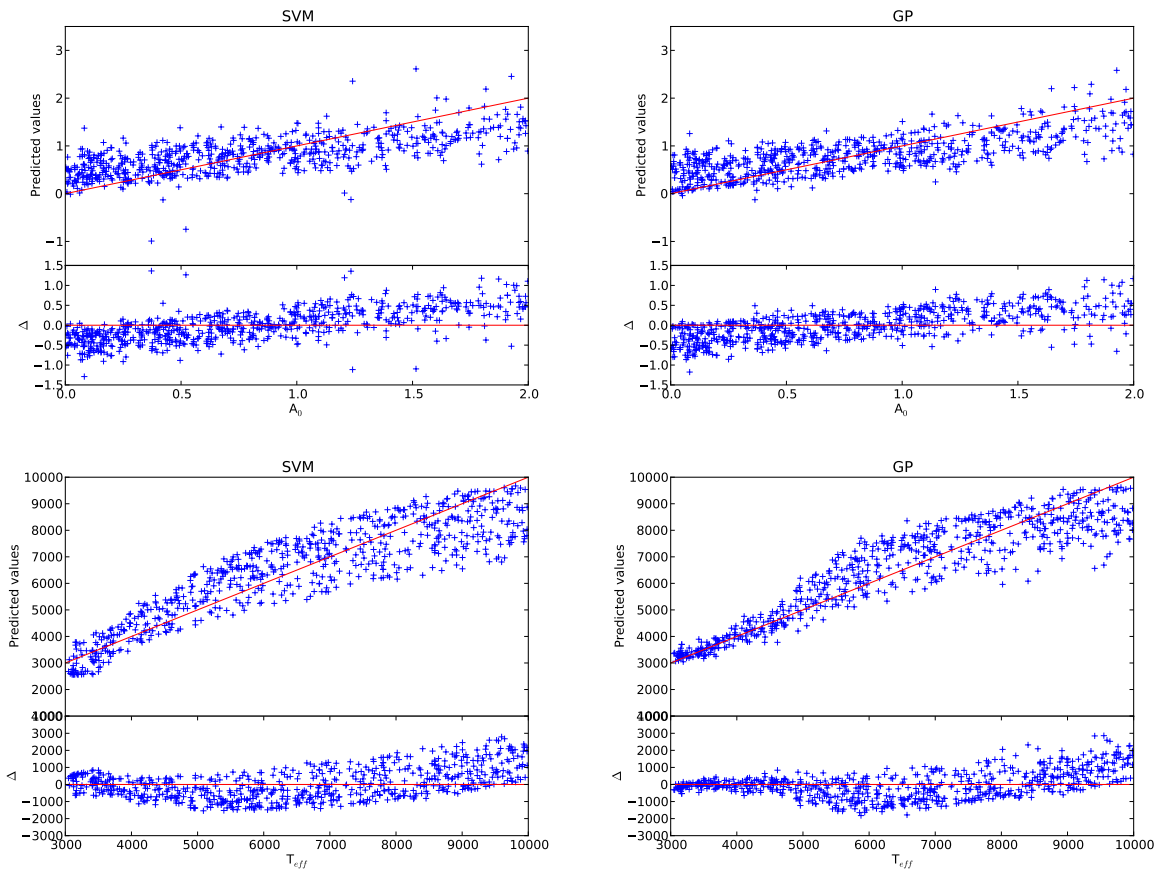


FIGURE 9: Test with uniformly distributed samples (see Figure 8). A scatter plot of the true APs and the predicted APs. In each subplot, top panel shows a relation between them and the bottom plot shows residuals (i.e. true - predicted). The red line in the top panel is a function of $y = x$ and the red line in the bottom panel is function of $y = 0$. Top left: extinction estimation using SVM, top right: extinction estimation using GP, bottom left: temperature estimation using SVM, and bottom right: temperature estimation using GP.

TABLE 7: Performance using uniformly distributed samples

Method	AP	RMSE	MAE
SVM	extinction	0.41 (mag)	0.33 (mag)
	temperature	900 (K)	727 (K)
GP	extinction	0.38 (mag)	0.30 (mag)
	temperature	787 (K)	595 (K)

TABLE 8: Prior-only MAE

extinction	temperature
0.49	1748.70

Prior-only MAE which can be understood as the upper limit of errors.

3.4.3 Extrapolated Application to Samples of Extinction > 2.0 mag and of High Temperature > 10,000K

Although the models were trained on the samples of extinction < 2.0 mag and of temperature < 10,000 K, we tried to apply the models to the samples of extinction > 2.0 mag and of high temperature > 10,000 K. It is expected that the predicted APs would not be very useful since the models are not trained on samples of these AP ranges. Nevertheless, we can at least tell how badly the trained models would predict for those sources (Table 9). We show the prediction results for the sample in Figure 10 . As the tables and the figure shows, the predicted APs are not very useful at all. Therefore in order to properly predict APs of these ranges, new models should be trained on samples of these ranges. Nevertheless we are not yet trained such models, which might be done in the near future.

3.5 Application of Prior

In this section, we present preliminary results using extinction and temperature priors. The priors we used for this test might be incomplete and thus the results could be biased to the priors. Nevertheless, in the case of insufficient input data such as this work estimating APs using only three (two) colors, appropriate selection of priors could improve results. Note that we can always update or even drop the priors when it is necessary. In addition it is worth mentioning that applying prior means we need to derive a likelihood, which eventually gives posterior. Note that we can derive uncertainty of the predicted APs using posterior, which is not available to derive from SVM models themselves.

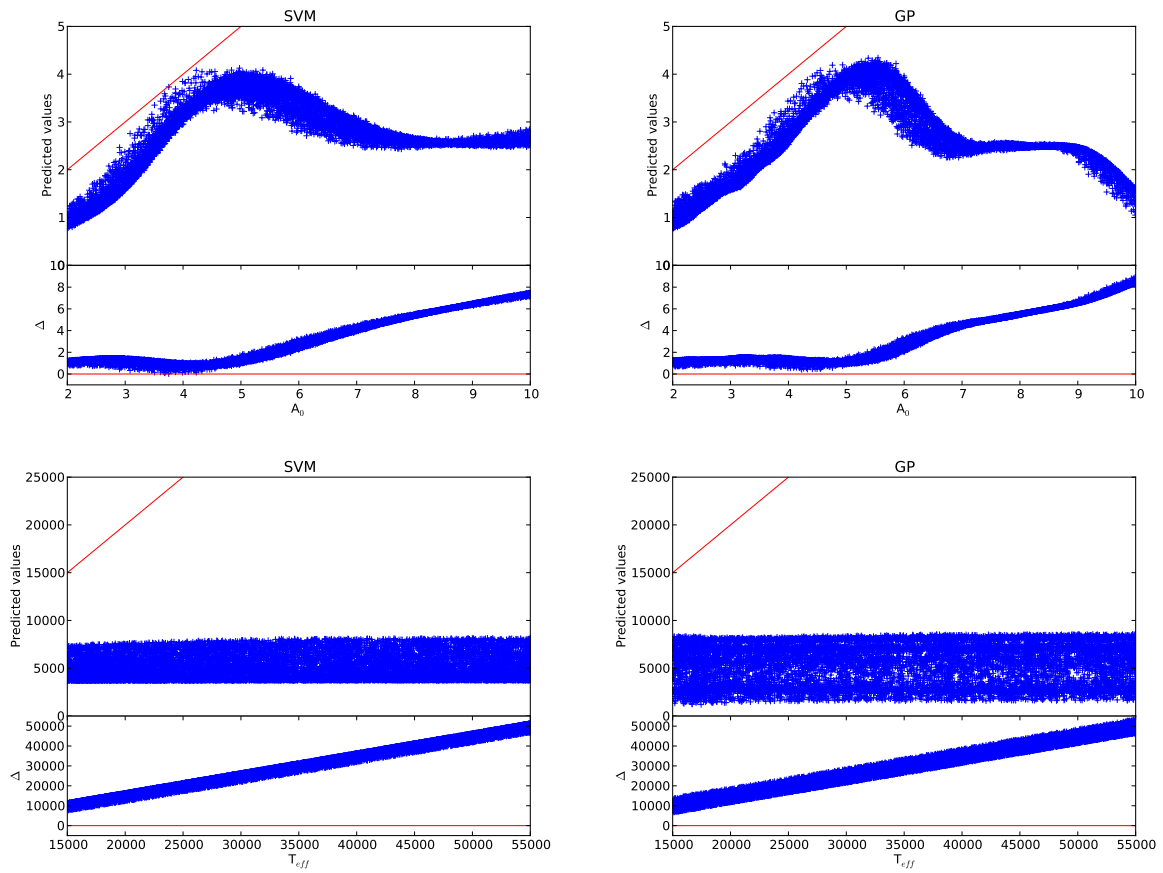


FIGURE 10: **Extrapolated Results:** test with samples of extinction > 2.0 mag and of temperature $> 10,000$ K, where the *train data does not cover* at all. A scatter plot of the true APs and the predicted APs. In each subplot, top panel shows a relation between them and the bottom plot shows residuals (i.e. true - predicted). The red line in the top panel is a function of $y = x$ and the red line in the bottom panel is function of $y = 0$. Top left: extinction estimation using SVM, top right: extinction estimation using GP, bottom left: temperature estimation using SVM, and bottom left: temperature estimation using GP.

TABLE 9: **Extrapolated Results:** Performance for samples of extinction > 2.0 mag and of temperature $> 10,000$ K

Method	Library	AP	RMSE	MAE
SVM				
	OB	extinction	3.30 (mag)	2.80 (mag)
		temperature	31649 (K)	1774 (K)
	A	extinction	3.39 (mag)	2.80 (mag)
		temperature	6863 (K)	1774 (K)
GP				
	OB	extinction	3.46 (mag)	3.49 (mag)
		temperature	31454 (K)	2604 (K)
	A	extinction	3.74 (mag)	3.49 (mag)
		temperature	7026 (K)	2604 (K)

3.5.1 Likelihood

To derive likelihood, we first calculated the mean value and the standard deviation value of predicted APs for a certain range of the true APs (windows) under the assumption that the distribution of the predicted APs is a normal distribution. These values are calculated using the data shown in Figure 7. We then defined W_i using the calculated quantities as:

$$W_i \equiv N(\mu_{i,predicted}; \sigma_{i,predicted}) \quad (3)$$

where i is the index of each window, $\mu_{i,predicted}$ and $\sigma_{i,predicted}$ are derived from Figure 7. Figure 11 shows 1) the difference between the mean values of true and predicted APs (the blue squares) for each window, and 2) standard deviation values of predicted APs (the error bars), along the true APs (x-axis). The interval between data points (the blue squares) are irregular because we collected at least 50 measurements to calculate the mean and standard deviation values. As the figure shows, the standard deviation values are quite big ($\overline{\sigma_{\Delta A_0}} \sim 0.33$ mag, $\overline{\sigma_{\Delta T_{eff}}} \sim 628$ K).

Using W_i , we can determine likelihood, L , for a predicted AP by calculating a score at each W_i as:

$$L = P(AP_{predicted}|AP_{true}) = N(S_i) \quad (4)$$

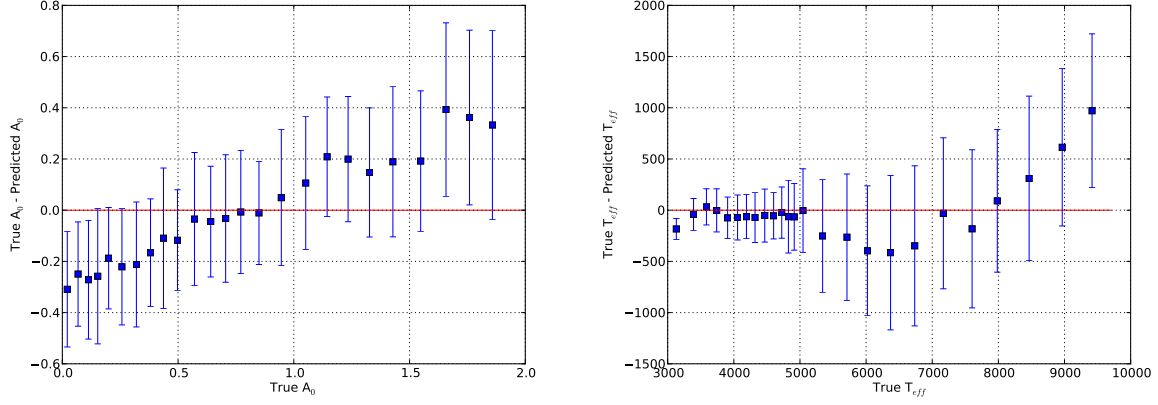


FIGURE 11: Likelihood of extinction and temperature.

where i is the index of each window, N is the standard normal distribution, $N(0, 1)$, and the score, S_i , is calculated by:

$$S_i = \frac{AP_{predicted} - \mu_{i,predicted}}{\sigma_{i,predicted}} \quad (5)$$

Figure 12 shows one example of likelihood, L , (shown in yellow lines) for a given predicted extinction (left panel) and temperature (right panel). L is scaled so that the integral value in the AP range is one. As can be expected, L is not exactly normally distributed. For the case of temperature, it seems that it is normally distributed. The reason for this is because the ΔT_{eff} at the lower temperature is quite small as shown in the right panel of Figure 11. The blue dashed line is the predicted value and the red dashed line is the true value. We will get back to this figure later in the following sections to explain details. We show two more examples at Figure 13 and 14.

3.5.2 Realistic Prior for Extinction and Temperature

To derive the extinction prior, we employed the data from Arenou et al. (1992) that provides a table of parameters for extinction estimation at a certain position (l, b) in our Galaxy. For this preliminary test, we assumed that all the stars are located at 1kpc away from the Sun.³ The left panel of Figure 15 shows the derived extinction map. Using the extinction map and (l, b) of each star, we can estimate an extinction at a certain position. We then can assume the distribution of extinction at that position as Gamma distribution which is monotonically decreasing.

In the case of temperature prior, we used a temperature distribution from the Gaia Universe

³ Arenou et al. (1992)'s results are valid up to 1kpc.

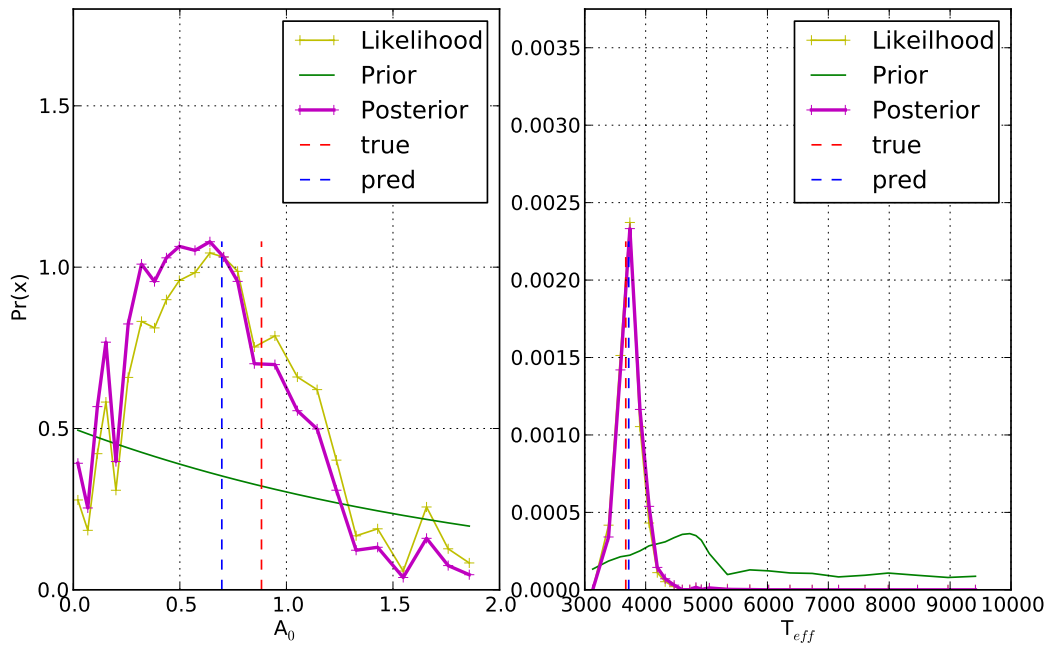


FIGURE 12: Likelihood (L), prior, and posterior distribution.

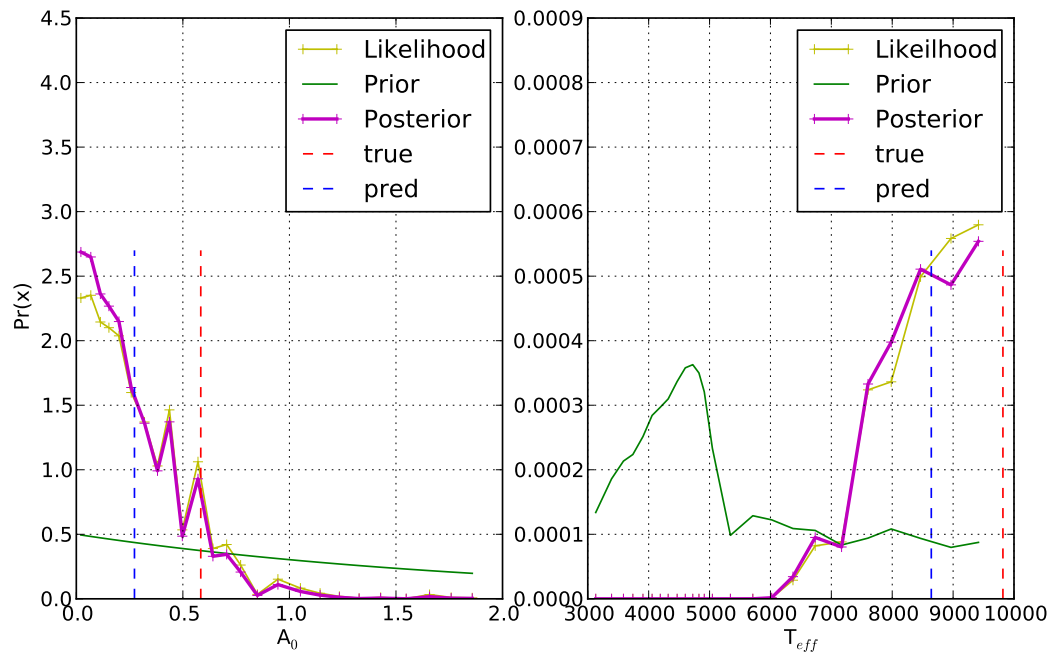


FIGURE 13: Likelihood (L), prior, and posterior distribution.

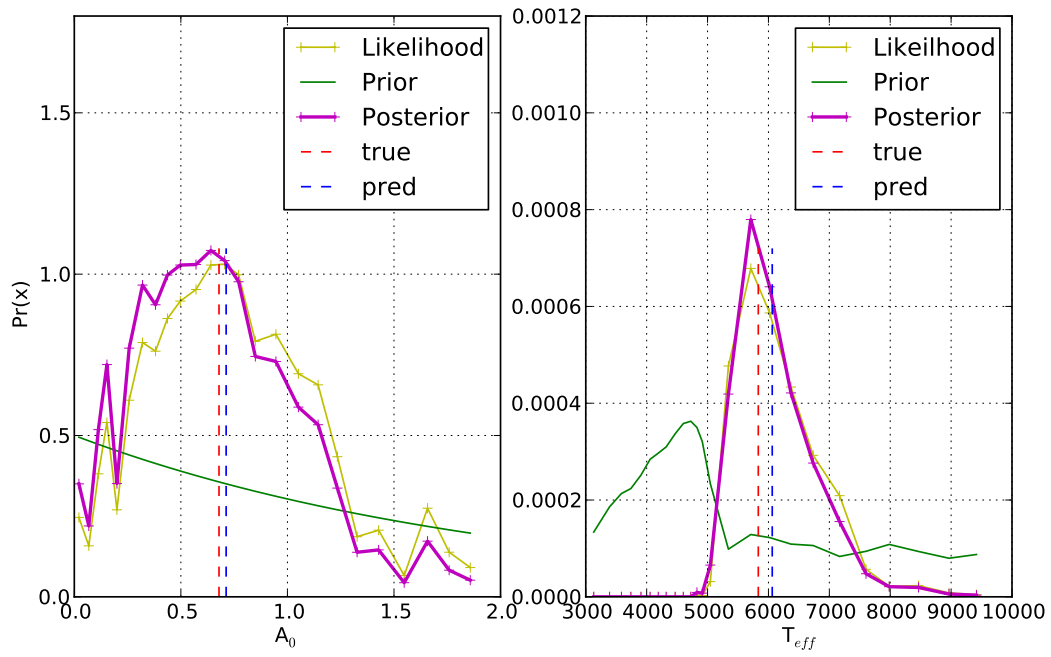


FIGURE 14: Likelihood (L), prior, and posterior distribution.

Model Statistics v.10 (XL-028, Robin et al. 2012). For the test, we extracted the distribution of temperature for stars of $G \sim 15$ (right panel in Figure 15). We then interpolated the histogram using a smoothed spline (red line). We normalized the interpolated line so that the integral is one.

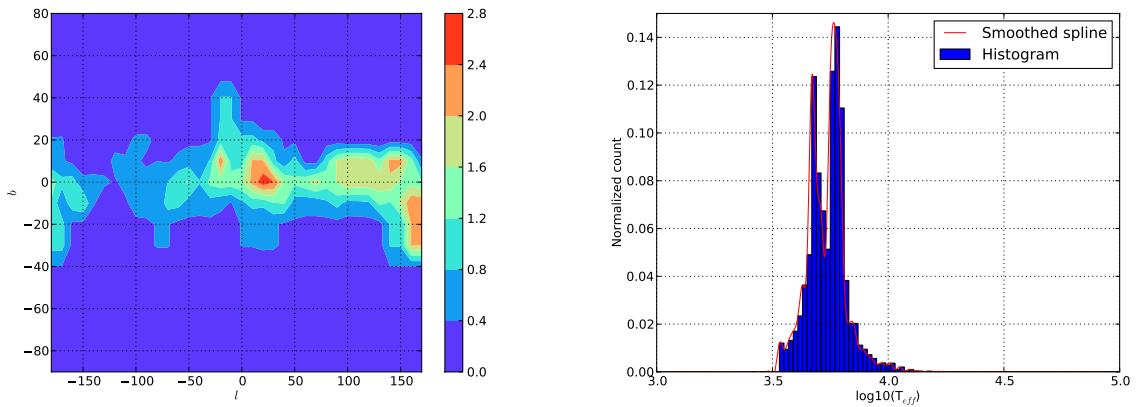


FIGURE 15: left: extinction map generated using (Arenou et al., 1992). Right: temperature prior derived from Gaia Universe Model Statistics (GUMS) v.10 (XL-028, Robin et al. 2012).

3.5.3 Experimental Prior for Extinction and Temperature

Although we could use rather realistic priors for extinction and temperature explained in the previous section, it does not mean that applying these priors would improve the results because:

- the dataset that we used for this test (i.e. PHOENIX RAN LIB1) randomly generated extinction for each source regardless of its spatial coordinates (i.e. l and b) while the extinction prior we introduced in the previous section depends on spatial coordinates. Thus extinction values of the realistic prior are generally way off from those of dataset.
- the temperature prior that we extracted from GUMS (XL-028, Robin et al. 2012) is a distribution for all stellar sources, not only for PHOENIX RAN LIB1.

Therefore we decided to generate alternative priors for this test (hereinafter, experimental priors). For extinction prior, we used the Gamma distribution. For temperature prior, we used the distribution of the training data. We first interpolated the histogram of temperature from the training data using a smoothed spline, and normalized the interpolated function so that the integral is one. Figure 12 shows the generated priors for each AP (green line in left and right panel).

3.5.4 Posterior

Finally, we calculated the posterior using the likelihood and the experimental priors mentioned in the previous sections as:

$$P(AP_{true}|AP_{predicted}) = \frac{1}{Z} L P \quad (6)$$

where L is the likelihood defined in Equation 4, P is the experimental prior introduced in Section 3.5.3, and Z is a normalization constant. We calculate the normalization constant by calculating integral value of the posterior through the AP ranges. Figure 12, 13 and 14 show examples of posteriors for each AP (magenta line). After we applied the priors, we calculated few statistics using all test data shown in Table 10. MAE in the table is defined as:

- without prior: an average value of MAEs between mean values of *likelihood* distribution and the true APs
- with prior: an average value of MAEs between mean values of the *posterior* distribution and the true APs

Precision is defined as

- without prior: an average standard deviation value of *likelihood* distribution
- with prior: an average standard deviation value of *posterior* distribution

In addition, we defined an alternative likelihood, L_{alt} , shown in the left panel of Figure 17. L_{alt} is a normal distribution with mean of [predicted T_{eff} , predicted A_0] and with a covariance matrix shown in Figure 16, which thus can be understood as a typical likelihood. To calculate the covariance matrix, we first derived ΔT_{eff} versus ΔA_0 (as shown in Figure 16), we then fitted the data with multivariate normal distribution. The derived covariance matrix is:

$$\begin{pmatrix} 394784.77 & 181.81 \\ 181.81 & 0.11 \end{pmatrix}$$

The standard deviation value for ΔT_{eff} is $\sim 628K$ and for ΔA_0 is ~ 0.33 mag. Note that although we assumed the normal distribution to calculate the covariance matrix, the actual distribution shown in Figure 16 are not really normal distribution. This could degrade the results when using the covariance matrix. It is worth mentioning that we could improve L_{alt} as well

by calculating multiple covariance matrices along the AP ranges (such as how we derived W_i at Equation 3), which eventually will show similar behavior with L (Equation 4). However note that deriving posterior using such likelihood is computationally more expensive.

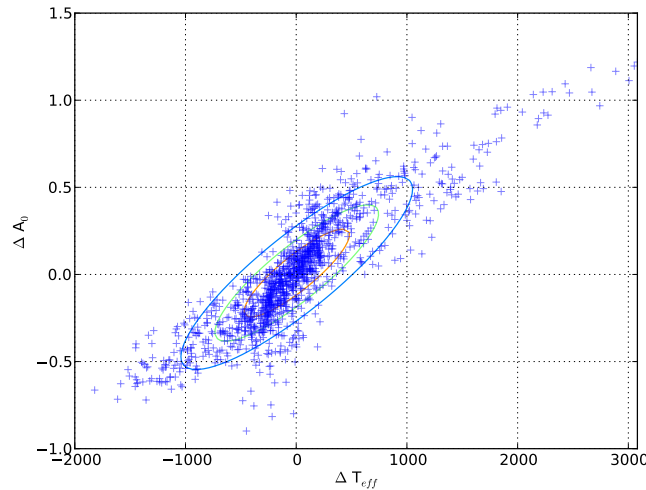


FIGURE 16: Scatter plot of ΔT_{eff} versus ΔA_0 . The blue plus are data points. The covariance matrix (contour) was derived by fitting multivariate normal distribution.

Nevertheless, Figure 17 shows one example using L_{alt} and the realistic priors. The yellow square is the predicted AP and the yellow diamond is the true AP. The different colored contour indicates different confidence levels of L_{alt} . The right panel is the result after applying the realistic priors for both extinction and temperature. As expected, the overall results are not improved since the realistic priors do not match very well with the data. Table 11 shows few statistics. The results are not any better than the results using the experimental priors shown in Table 10. Let's examine Table 11 and 10 in a little more details.

- Extinction: the average MAEs without prior are close to each other since mean values of likelihood of two cases should be similar regardless of which definition we used to generate the likelihoods. However, showing similar average MAEs does not mean that the two likelihood are identical. Remember that we use a single covariance matrix to generate L_{alt} shown in Figure 17, but the other likelihood (L) is generated by binned data (Equation 4 and Figure 12). Thus L could show better performance at some region such as at the lower temperature (see right panel in Figure 11 and Figure 12) while L_{alt} will always show averaged performance for the whole range of AP parameters.

Nevertheless, after applying extinction priors, either the average MAE values or precision values did not improved at all which indicates our definition of prior is

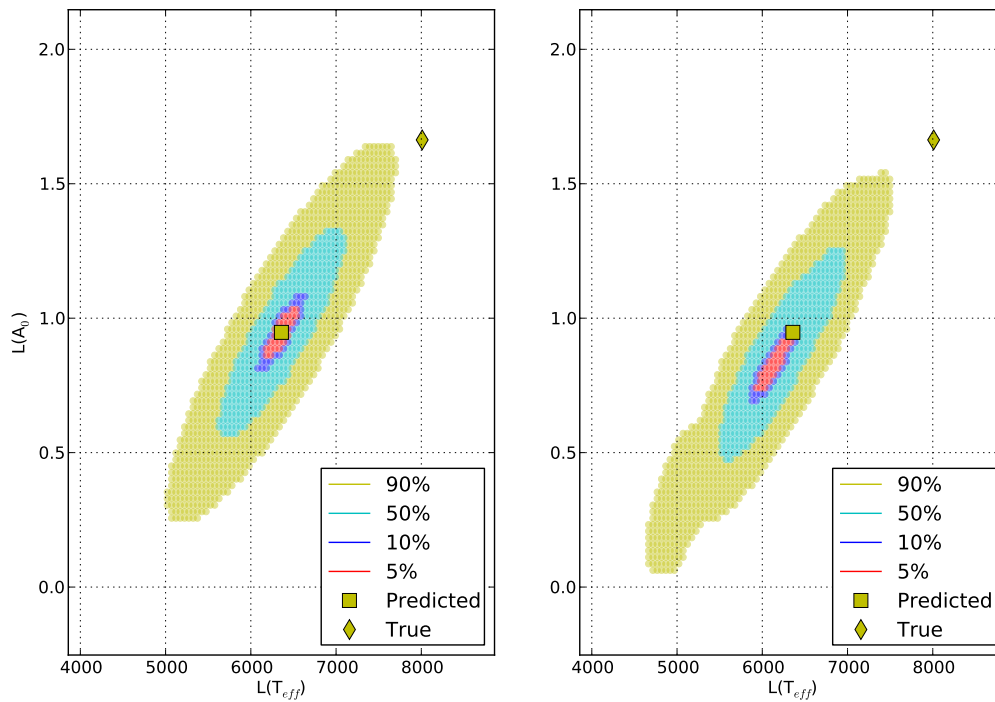


FIGURE 17: Left: likelihood distribution. Right: after applying both temperature and extinction priors.

TABLE 10: Performance Using Experimental Prior and Likelihood, L shown in Equation 4

AP		Without prior	With prior
Extinction	MAE	0.28 (mag)	0.28 (mag)
	Precision	0.32 (mag)	0.31 (mag)
Temperature	MAE	542 (K)	542 (K)
	Precision	606 (K)	587 (K)

TABLE 11: Performance Using Realistic Prior and Likelihood, L_{alt} introduced in Section 3.5.4

AP		Without prior	With prior
Extinction	MAE	0.29 (mag)	0.37 (mag)
	Precision	0.33 (mag)	0.26 (mag)
Temperature	MAE	522 (K)	671 (K)
	Precision	627 (K)	534 (K)

not really practical or effective. Thus it seems that we need more comprehensive and practical priors for further improvements.

- Temperature: The results can be understood as same as the extinction cases.

4 Implementation

So far, the tests shown in this TN have been done mostly using Python. The implementation of either partial or full portion of this work into GSP-phot will be made soon and deliver at the next CU8 software delivery scheduled at the end of May, 2013. Here is brief summary of the implementation plan:

- MainDelivery3 PHOENIX RAN1 library will be used.
- individual models for different magnitude and different APs (i.e. extinctions and temperature) will be trained.
- three and two color models will be separately trained.

- noise will be added to BP/RP spectra..
- hyperparameter tuning will be done using brute-force search.
- to reduce training time, the training processes will be parallelized.

5 Conclusion and Discussion

We tested two machine learning methods to estimate two APs including extinctions and temperature using three color information extracted from MainDelivery3 PHOENIX RAN1 cycle8 library. The three colors are $G_{Mag} - G_{BP}$, $G_{Mag} - G_{RP}$ and $G_{Mag} - G_{RVS}$. We also predicted APs using only two colors (i.e. $G_{Mag} - G_{BP}$ and $G_{Mag} - G_{RP}$), which might be useful for faint stars that would not have G_{RVS} .

The predicted APs would be useful for the Gaia community when no BP and RP spectra are available at the early stage after the launch of the Gaia satellite, thus when accurate extinction or temperature information cannot be provided.

On the basis of these experiments shown in this TN, we will implement a Java package for few band AP estimation, which we named as: **Priam - Photometric Estimation of Astrophysical Parameters**.

References

- Arenou, F., Grenon, M., Gomez, A., 1992, A&A, 258, 104, [ADS Link](#)
- [**CBJ-064**], Bailer-Jones, C., 2012, *Minutes of the tenth CU8 meeting*,
GAIA-C8-MN-MPIA-CBJ-064,
URL <http://www.rssd.esa.int/lmlink/livelink/open/3120734>
- Bailer-Jones, C.A.L., 2011, MNRAS, 411, 435, [ADS Link](#)
- Bishop, C.M., 2006, *Pattern recognition and machine learning*, Springer, 1st ed. 2006. corr. 2nd printing edn.
- Cortes, C., Vapnik, V., 1995, Machine Learning, 20, 273,
URL <http://dx.doi.org/10.1007/BF00994018>,
10.1007/BF00994018
- Jones, D.O., West, A.A., Foster, J.B., 2011, AJ, 142, 44, [ADS Link](#)
- Liu, C., Bailer-Jones, C.A.L., Sordo, R., et al., 2012, MNRAS, 426, 2463, [ADS Link](#)

TABLE 12: Performance of AP estimations using BP and RP spectra

Method	AP	MAE
SVM		
	extinction	0.04 (mag)
	temperature	59 (K)
ILIUM		
	extinction	0.09 (mag)
	temperature	110 (K)
Aeneas (p-model)		
	extinction	0.07 (mag)
	temperature	72 (K)
Aeneas (pq-model)		
	extinction	0.07 (mag)
	temperature	71 (K)

Performances from the table 2 of Liu et al. (2012).

[**XL-028**], Luri, X., Isasi, Y., Borrachero, R., et al., 2012, *Gaia Universe Model Statistics - version 10*,
 GAIA-C2-TN-UB-XL-028,
 URL <http://www.rssd.esa.int/l1link/livelink/open/3110371>

Rasmussen, C.E., Williams, C., 2006, *Gaussian Processes for Machine Learning*, MIT Press,
 URL <http://www.gaussianprocess.org/gpml/>

Robin, A.C., Luri, X., Reylé, C., et al., 2012, *A&A*, 543, A100, ADS Link

Appendix

In order to compare our results in Table 3 with the work done by (Liu et al., 2012) which used BP and RP spectra to estimate APs, we show the MAE of the work in Table 12. As the table clearly shows, the performance using BP and RP spectra surpasses the performance using three colors. This is expected results since BP and RP spectra have much more information than three colors.